Passage of Bolides through the Atmosphere

O. Popova

Abstract Different fragmentation models are applied to a number of events, including the entry of TC_3 2008 asteroid in order to reproduce existing observational data.

1 Introduction

Fragmentation is a very important phenomenon which occurs during the meteoroid entry into the atmosphere and adds more drastic effects than mere deceleration and ablation. Modeling of bolide fragmentation $(100 - 10^6$ kg in mass) may be divided into several approaches. Detail fitting of observational data (deceleration and/or light curves) allows the determination of some meteoroid parameters (ablation and shape-density coefficients, fragmentation points, amount of mass loss) (Ceplecha et al. 1993; Ceplecha and ReVelle 2005). Observational data with high accuracy are needed for the gross-fragmentation model (Ceplecha et al. 1993), which is used for the analysis of European and Desert bolide networks data. Hydrodynamical models, which describe the entry of the meteoroid including evolution of its material, are applied mainly for large bodies ($>10^6$ kg) (Boslough et al. 1994; Svetsov et al. 1995; Shuvalov and Artemieva 2002, and others). Numerous papers were devoted to the application of standard equations for large meteoroid entry in the attempts to reproduce dynamics and/or radiation for different bolides and to predict meteorite falls. These modeling efforts are often supplemented by different fragmentation models (Baldwin and Sheaffer, 1971; Borovička et al. 1998; Artemieva and Shuvalov, 2001; Bland and Artemieva, 2006, and others).

The fragmentation may occur in different ways. For example, few large fragments are formed. These pieces initially interact through their shock waves and then continue their flight independently. The progressive fragmentation model suggests that meteoroids are disrupted into fragments, which continue their flight as independent bodies and may be disrupted further. Similar models were suggested in numerous papers, beginning with Levin (1956) and initial interaction of fragments started to be taken into account after the paper by Passey and Melosh (1980). The progressive fragmentation model with lateral spreading of formed fragments is widely used (Artemieva and Shuvalov, 1996; Nemtchinov and Popova, 1997; Borovička et al. 1998; Bland and Artemieva, 2006).

The second mode of fragmentation is the disruption into a cloud of small fragments and vapor, which are united by the common shock wave (Svetsov et al. 1995). This fragmentation occurs during the disruption of relatively large bodies. If the time between fragmentations is smaller than the time for fragment separation, all the fragments move as a unit, and a swarm of fragments and vapor penetrates deeper, being deformed by the aerodynamical loading like a drop of liquid (Hills and Goda 1993 and others). This liquid-like or "pancake" model assumes that the meteoroid breaks up into a swarm of small

O. Popova (✉)

Institute for Dynamics of Geospheres Russian Academy of Sciences, Leninsky prospect 38, bldg.1, Moscow 119334, Russia. Phone: +7 495 939 70 00; Fax: +7 499 137 65 11; E-mail: olga@idg.chph.ras.ru

bodies, which continue their flight as a single mass with increasing pancake-like cross-section. The smallest fragments can be evaporated easily and fill the volume between larger pieces. Initially formed fragments penetrate together deeper into the atmosphere and the fragmentation proceeds further. But large fragments may escape the cloud and continue the flight as independent bodies.

The formation of a fragment–vapor cloud was observed in the breakup of a meteoroid on 1 February 1994 (McCord et al. 1995), in the fragmentation of the Benesov bolide (Borovička et al. 1998), and in other cases. The total picture of fragmented-body motion is comparatively complicated. Both scenarios are realized in the real events (Borovička et al. 1998).

2 The Entry of TC$_3$ 2008

2.1 Observational Data

The entry of asteroid TC$_3$ 2008 over Sudan was observed by numerous eyewitnesses and a few detecting systems, including Meteosat satellites (Borovička and Charvat, 2009), infrasonic array and US Government satellites (Jenniskens et al. 2009). Meteorites named Almahata Sitta were recovered in December 2008. Meteorite searches allowed collectors to find about 300 fragments with total mass up to 3.95 kg (Jenniskens et al. 2009). Masses (from 1.5 g to 283 g) were found along a 29 km path.

Almahata Sitta was classified as an anomalous polymict ureilite (Jenniskens et al. 2009). Different lithologies including a number of non-ureilite fragments (enstatite and ordinary chondrites) were found among retrieved samples. All pieces are fresh and unweathered, so they probably had been incorporated into asteroid TC$_3$ 2008 and did not originate from an earlier meteor event (Bischoff et al. 2010). This indicates that the asteroid was probably a collection of different lithologies, which were included as distinct stones within the asteroid body. The measured bulk density of Almahata Sitta varies from fragment to fragment ($2.9 - 3.1$ g/cm^3) and porosity is about 15-20% (Kohout et al. 2010). These values are close to the typical ureilite values (3.05 g/cm^3 and 9%; Britt and Consolmagno, 2003). Welten et al. (2010) estimated the macroporosity of the asteroid as high as about 50%. One small piece of Almahata Sitta was disrupted in the laboratory and its measured tensile strength was about 56 ± 25 MPa (Jenniskens et al. 2009).

The initial diameter of this meteoroid was estimated as 4.1 ± 0.3 m based on asteroid visual magnitude (Jenniskens et al. 2009). Corresponding pre-atmospheric mass ($\rho = 2.3$ g/cm^3) is about 83 ± 2 5 t (Jenniskens et al. 2009). This estimate correlates well with the mass obtained based on infrasound signal (87 ± 27 t). The irradiated energy recorded by US DoD satellites allows an estimated initial mass of 56 t, assuming an integral luminous efficiency of 9.3% based on optical events calibrated by infrasound registration (Brown et al. 2002a). According to theoretical estimates (Nemtchinov et al. 1997) the integral luminous efficiency is slightly lower for this low velocity entry - 6.8-8.2%; these values result in initial mass of about 63-77 t.

The lower mass estimate (~20 t) is suggested by Kohout et al. (2010) and is based on assumptions of higher albedo and essential macroporosity of the asteroid. But this low mass estimate corresponds to very high value of integral luminous efficiency (~26%), which seems not probable.

The light curve recorded by US DoD satellites wasn't published, but it was released that the signal consisted of three peaks, while the most energy was radiated in the middle of a 1-s pulse at 37 km altitude and a final pulse 1 s later (at about 33 km altitude) (Jenniskens et al. 2009). Analysis of Meteosat 8 images allows the estimation of bolide brightness at two random heights, 45 and 37.5 km, where it reached −18.8 and −19.7 magnitude, respectively (Borovička and Charvat, 2009). The peak

brightness was probably brighter than -20^{mag} (Borovička and Charvat, 2009). A schematic version of possible light curve is shown on Figure 1. Minimal detectable intensity is assumed to be about 2 10^9 W/sr. Shapes of light peaks are arbitrary, but the total irradiated energy corresponds to reported value of 4 10^{11} J (or 0.096 kt; USAF press release).

Analysis of Meteosat 8 images allows the conclusion that dust release due to meteoroid breakup occurred at altitudes 44, 37 and possibly at 53 km. The broken pressures were estimated as 0.2-0.3 MPa (at 46-42 km altitude) and 1MPa (at 33 km) (Jenniskens et al. 2009).
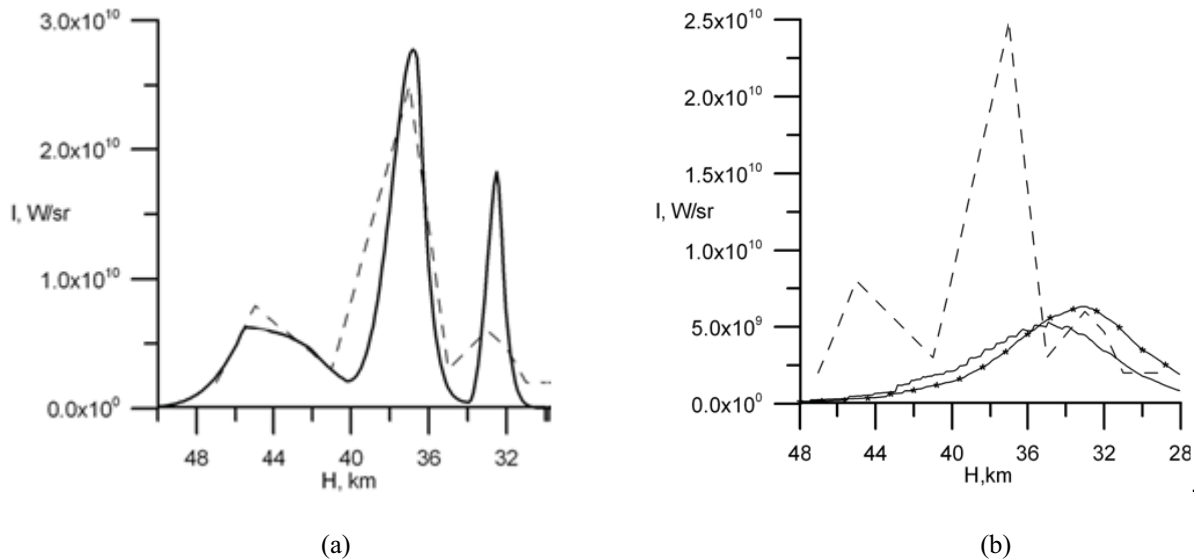

(a)   (b)

Figure 1. (a) Schematic light curve of Almahata Sitta (dashed line) and an example of model light curves of Almahata Sitta in the frame of pan-cake model. (b) Schematic light curve of Almahata Sitta (dashed line) and model curves obtained in the frame of disruption onto two fragments (pointed line) and disruption into a number of fragments.

2.2 Modeling Efforts

2.2.1 Pan-cake Model

The presence of three peaks in the Almahata Sitta light curve indicates that there were three main stages of fragmentation. Similar light curves for a number of satellite observed bolides were successfully reproduced in the frame of pan-cake (or liquid-like) models (Svetsov et al. 1995; Nemtchinov et al. 1997; Popova and Nemtchinov 2008). Although liquid like models mentioned above are applicable mainly for large impactors, which are destroyed so intensively that fragments couldn't be separated (>~4-10 m in size) (Svetsov et al. 1995; Bland and Artemieva 2006), its modifications provide reasonable energy release. These models may be suitable for catastrophic disruption, when a huge number of fragments are formed.

The shape of light curve depends on chosen model parameters (rate of dust cloud spreading, mass fraction fragmented in every break up, assumed strength at the breakup). One possible light curve of Almahata Sitta is shown on Figure1a. The meteoroid with initial mass of 83 tons and bulk density 2.5 g/cm^3 initially disintegrated at the altitude of about 50.4 km under the aerodynamical loading about 0.15

MPa on two-three big pieces and a cloud of small fragments and dust, which may be described in the frame of pan-cake model. Formation of this cloud is accompanied by the first flare in the light curve. The next fragment (or few fragments) is broken up by aerodynamical loading of about 0.6 MPa at 40.2 km altitude. And the last fraction of meteoroid was disrupted at 33.9 km altitude under loading of about 1.5 MPa. The fractions of initial mass fragmented at different altitudes are roughly 33, 47 and 20% (i.e. ~27.6, 38.4 and 16 t). The integral luminous efficiency was about 6.5%, corresponding to a total irradiated energy of about 0.099 kt. Slightly different values of mass fractions (25, 65 and 10 %) and strengths (0.15, 0.4 and 1.5 MPa) also permits reproduction of the triple peaked light curve. About 70% of the initial mass is evaporated, and about of 30% of it (~25 t) remains in the atmosphere as a decelerated cloud of dust.

According to the statistical strength theory (Weibull, 1951) and direct observations on natural rocks (e.g., Hartmann, 1969) the strength of a body in nature tends to decrease as body size increases. The effective strength is usually expressed as $\sigma = \sigma_s(m_s/m)^\alpha$, where σ and m are the effective strength and mass of the larger body, σ_s and m_s are those of small specimen, and α is a scaling factor. There are no precisely determined values of scaling factor α, but for stony bodies the exponent is estimated to be in the range of 0.1–0.5 (Svetsov et al. 1995). It has not been proven that theses values hold for meteorite strength, though that is commonly assumed in meteoroid fragmentation theories (e.g., Baldwin and Sheaffer, 1971; Tsvetkov and Skripnik, 1991; Nemtchinov and Popova, 1997; Borovička et al. 1998; Artemieva and Shuvalov, 2001; Bland and Artemieva, 2006).

The inferred strength at breakups depart from the values, which are predicted by the strength scaling law with exponent $\alpha \sim 0.25$. Bland and Artemieva (2006) suggest using a small variation in strength (about 10% around predicted values), but there is much more significant deviation. Even application of larger variations in strength (up to 50% of predicted value) reproduces only double peak curves, and the altitude difference between peaks is smaller than observed one.

The pan-cake model is not capable of providing a mass-velocity distribution of meteoroid fragments; it cannot predict the meteorite strewn field. Besides, the same luminous efficiency is used for the solid fragment and for the cloud of vapor if their sizes are equal.

2.2.2 Progressive Fragmentation Models

The possibility to describe the fate of individual fragments, to determine meteorite strewn or crater fields is the main and extremely important advantage of the progressive fragmentation type models. The number of fragments changes in the process of the disruption from 1 (a parent body) to an arbitrarily large value, depending on the assumed properties of the meteoroid. These types of models usually incorporate the strength scaling law mentioned above and different assumptions about distribution of formed fragments on mass.

Bland and Artemieva (2006) suggested that each fragmentation of a single body results in two fragments with smaller mass and usually higher strength (although a small (<10%) variation in strength was considered). Each fragment is subjected to additional fragmentations later if the dynamic loading exceeds the updated fragment strength.

Disruption into two fragments supplemented with the strength scaling law leads to a single peak light curve. Corresponding modeling efforts are shown on Figure 1b. An initial meteoroid mass $m_s \sim 83$ tons, initial strength $\sigma_s \sim 0.15$-0.2 MPa and $\alpha \sim 0.25$ are assumed. The observed value of strength at initial breakup is used as sample strength. The usage of stony meteorite sample strength (~30MPa for 0.01 kg) results in higher initial strength and lower altitude of fragmentation beginning (~40 km). Masses of daughter fragments are chosen randomly in every breakup. Heat transfer coefficient $C_h \sim 0.1$

corresponds to ablation parameter of about 0.016 s^2/km^2 similar to the characteristic value for stony bodies (0.014 s^2/km^2; Ceplecha et al. 1998) and to the value used by Bland and Artemieva (2006). The used luminous efficiencies in the satellite detectors passband were obtained in the course of radiative hydrodynamic numerical simulations (Golub' et al. 1996; Nemtchinov et al. 1997).

Fragmentation starts at 47 km altitude and proceeds down to about 29 km altitude. A large fraction of initial mass lands on the ground ($M_{fall} \sim 24$ t) in more than 5000 pieces. The largest fragment reaches 10-20 kg (size of largest fragment is mainly determined by suggested strength scaling law and entry velocity). Most of the fallen mass is contained in the largest fragments. The integral luminous efficiency is about 2.5 - 3% and total light energy in the satellite detectors passband is about 0.03 – 0.05 kt TNT. Obtained values vary slightly from one set of calculations to another due to random choice of fragment size at breakup, but they are close to each other on average. The light pulse starts and ends at lower altitudes than the schematic one for the real event, the model light intensity and total irradiated energy are lower.

The single disruption event may result in a number of fragments. The mass distribution of fragmented rocks is often described by a power law (Hartmann 1969; Fujiwara et al. 1989). The power law distribution was also used in the description of meteorites (Jenniskens et al. 1994; Hildebrand et al. 2006) and in modeling of meteoroid entry (Nemtchinov and Popova, 1997; Borovička et al. 1998). Following Hartmann (1969), the cumulative fragment distribution in the breakup is assumed $N \sim m^{-b}$, where N is the cumulative number of fragments of mass > m; b is the negative slope in a log(N)-log(m) plot. The slope holds the same if a logarithmic-incremental plot is used ($F \sim m^{-b}$, where F = number of fragment within a logarithmic increment, $d$log$m$). The value $b \sim 0.6$ is accepted (Hartmann 1969). Disruption into several groups of fragments is considered. The average mass in neighboring groups changes in $\sqrt{2}$ times. The size of the largest daughter fragment is chosen randomly in every breakup, the number of groups and number of fragments in a group are determined based on parent fragment mass and fragment distribution mentioned above. All other parameters are the same as in the previous case.

The formation of a number of fragments causes the appearance of flashes in the light curve and slightly shifts the light curve to higher altitude (Figure 1b). The total fallen mass is still close to previous case ($M_{fall} \sim 20$-24 t), but the fallen mass has wider distribution. The total number of fragments increases essentially up to $10^4 – 10^5$. Nevertheless, the Almahata Sitta entry is poorly described by this and previous approaches. The fallen mass is too huge and irradiated energy is small.

2.2.3 Luminous Efficiency

The model light curves and total irradiated energy are dependent on assumed values of luminous efficiency. In general, luminous efficiencies vary with meteoroid size, velocity, altitude of flight and meteoroid composition. The dependence of luminous efficiencies f in the satellite detectors passband on altitude is given on Figure 2 for H-chondrite meteoroids (Golub et al. 1996; Nemtchinov et al. 1997). Luminous efficiencies mainly increase with meteoroid size and velocity and become higher at lower altitudes (Figure 2). The values of luminous efficiencies for achondrite bodies probably differ from H-chondrite ones due to the different composition of vapor in the radiative volume. In the entry modeling, the same luminous efficiency is used for the solid fragment and for the cloud of vapor if their sizes are equal. The model, which allows the determination of these coefficients, also has some limitations (Golub' et al. 1996), but currently it provides the best known estimates of luminous efficiency f for satellite observed light curves.
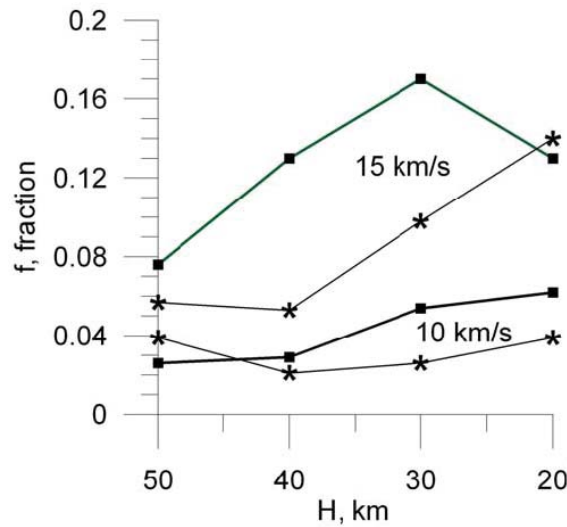
Figure 2. Luminous efficiencies for H-chondrite bodies versus altitude for two velocities (10 and 15 km/s) and two different sizes ($R \sim 0.14$ m (stars) and 1.4 m (squares))

Moreover, these luminous efficiencies were a basis for the determination of integral luminous efficiency η, i.e. the relation between total irradiated energy and initial kinetic energy for satellite observed bolides (Nemtchinov et al. 1997). An independent estimate of integral luminous efficiency η was obtained by Brown et al. (2002a) based mainly on infrasound registrations of 13 events. There were 3 meteorite falls among these events, compositions of other meteoroids were unknown (Brown et al 2002a). These estimates of η agree well with each other (Popova and Nemchinov 2008).

Roughly, it may be estimated that the light intensity has the precision of about two times. It should be also noted here that the light curve on Figure 1 is not really observed, it is only a sketch.

2.2.4 Hybrid Model

A large number of fragments may be formed simultaneously, but the progressive fragmentation model considers their flight and radiation independently. This type model deals better with few fragments, which are well separated. The progressive fragmentation model does not well describe the case of production of a large number of poor separated fragments. Different configurations of fragments may occur during the disruption process and influence further motion and radiation of fragments (Artemieva and Shuvalov, 1996, 2001). A number of separated fragments may be formed whereas smaller fragments and dust probably have no time to be separated and form a spreading cloud. The suggestion that randomly chosen part of mass in the break up forms an expanding cloud of dust causes the appearance of the flares on the light curve (Figure 3a) and the increase of radiated energy up to 0.04-0.07 kt TNT, but these values are still lower than observed ones. Shape of light pulse varies from one numerical run to another. The total fallen mass decreases down to 6-14 t in 10^3-10^5 fragments. Fallen mass is essentially overestimated. Larger fraction of mass should be converted into the dust in breakups.
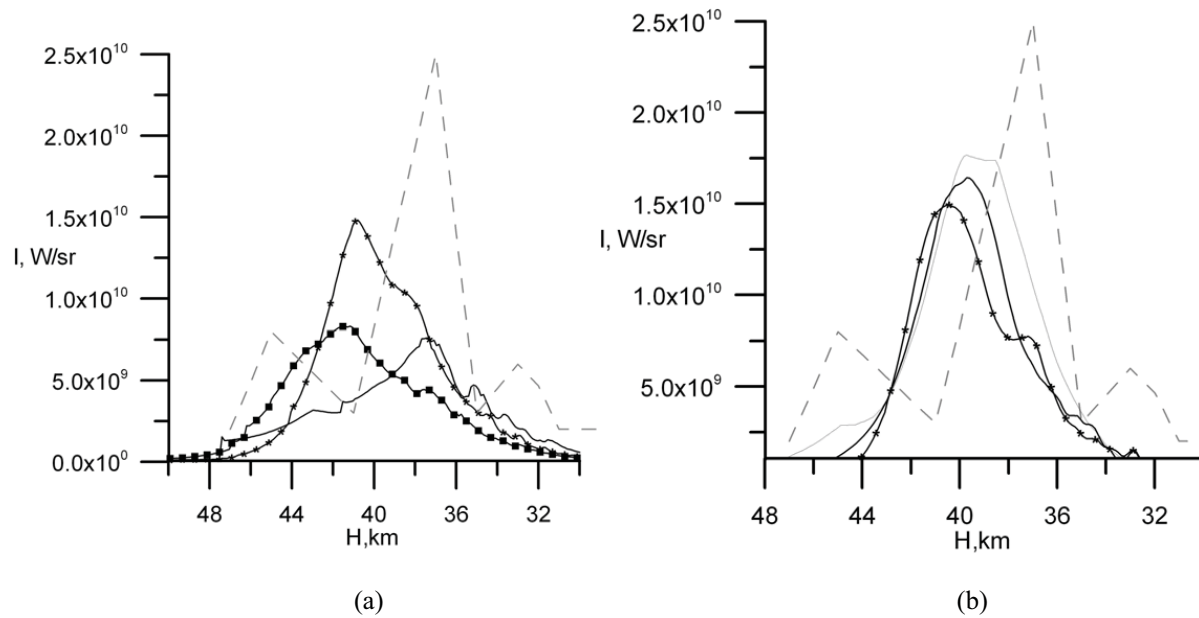
Figure 3. (a) Schematic light curve of Almahata Sitta (dashed line) and three model curves obtained under assumption that in every breakup some part of mass formed spreading cloud of vapor and dust. (b) Schematic light curve of Almahata Sitta (dashed line), two model curves obtained under assumption that in every breakup only few fragments are formed, some part of mass (~30% in average) formed spreading cloud (black and pointed curves); fragmentation onto two parts, one of which is converted into dust spreading cloud (gray curve).

During the progressive fragmentation of Moravka meteoroid (initial mass estimate ~1.2 ton) at the altitudes 30-40 km (Borovička and Kalenda, 2003) every break up of parent fragment resulted in formation of 1-3 relatively large fragments and dust (invisible on videorecord). Dust mass reached 10-90% of the parent fragment mass. Light curves obtained under the assumption that the number of fragments in the breakup is relatively small are shown on Figure 3b. Number of fragments in breakup is about 1-10 (2-3 in average) and some part of mass is converted into spreading dust cloud (~30% in average). Fallen mass in these cases is about 1.5-2.5 t, number of fragments is about 1000, integral luminous efficiency is about 4 – 5% and $E_r \sim$ 0.07-0.08 kt, but light pulse becomes more narrow (Figure 3b) even if the deviation of fragment strength from strength scaling law is allowed.

In the limiting case of the disruption into two parts – one fragment and dust cloud – the fallen mass decreases to about 5-15 kg in one piece. Integral luminous efficiency increases up to 5-6% and $E_r \sim$ 0.08 – 0.09 kt (Figure 3b). In order to get few peaks on the light curve the strength of fragments should essentially deviate from assumed strength scaling law, but the pulse is still narrow even if the strength may change on about 50% (Figure 3b).

It is possible to increase the mass fraction converted into dust clouds artificially and to fit observed light energy and shape of light pulse, but it is done above in the frame of pan-cake model. Light curve may be fitted if fallen mass is smaller about 100-400 kg, which seems to be an upper estimate.

3 Comparison With Other Events

3.1 Dust Formed in the Breakups

As it was mentioned above (Section 2.1), formation of dust clouds were directly observed during the entry of TC_3 2008 (Borovička and Charvat 2009). The amount of warm decelerated dust was estimated as at least 10 t, that is in the same order as our estimates (~25 t).

The Almahata Sitta entry confirmed that a large part of stony meteoroid mass and energy may be deposited in the atmosphere during the entry. Dust clouds are often observed at breakup events during observations of meter-sized meteoroids. These clouds are formed typically at 30-60 km altitude, but the data on particle size and on the mass fraction of the parent body, which was dispersed into dust, are scarce.

Attempts to collect dust from meteoroid disruption were done for two separate events, Revelstoke and Allende. The air through which a fireball had been observed to pass was sampled for meteoritic debris. Particulate matter was collected on special filters, which was mounted on aircraft and flown downwind from the site of the meteorite fall at 10-12 km altitude (Carr, 1970). According to Carr (1970), Revelstoke and Allende represented two different types of events. In the case of Revelstoke (type I carbonaceouse chondrite, corresponding sound wave energy is estimated as 10^{12}-10^{13} J, i.e.~1 kt) only a small 1 g of material was found in the fall area (possibly the result of rough terrain in the fall area, but may be the result of essential breakup in the atmosphere), large amount of debris still present in the atmosphere three days after event. Air samples contained a substantial excess over background of magnetite and transparent glass spherules and in addition contained a substantial number of irregular opaque particles high in Ni. Sizes of collected particles were mainly 2-4 μm (<10-25 μm). The Allende event was quite different (type III carbonaceouse chondrite, initial mass estimate >2000 kg, intial energy ~10^{12} J) >500 kg was found on the ground. Allende filters were clean – only a small number of particles were collected. The difference between sample and background is less than a factor of four, although some amount of opaque and glass spherules (<10 μm) were collected. Carr (1970) suggested that the difference in collected air samples and on fall sites resembles two different types of meteoroid breaks in the atmosphere.

A dust cloud formed due to fragmentation of large meteoroid (initial mass estimate 600 - 1900 t) was recorded during routine lidar observation of the atmosphere (Klekociuk et al. 2005). The meteoroid was fragmented at 32 km altitude and a dust cloud was recorded 7.5 hours later. The total mass of dust in this cloud was estimated as about 1000 t (that is lower estimates, because according to satellite observations, second fragmentation of meteoroid occurred at 25 km altitude). Dust size and concentration were estimated as 0.4-0.98 μm and 2-6 10^6 м$^{-3}$. Data on this event suggests that a large fraction of initial meteoroid mass may be released in the atmosphere as dust. Micron-sized particles may exist in the atmosphere during weeks-months and may play an important role both in climate processes and ozone layer dynamics (Klekociuk et al. 2005). No material was collected or found.

3.2 Tagish Lake and Carancas

The fraction of initial mass recovered as meteorites is mainly about f_m ~ 0.1-3 % for 11 meteorite falls with detailed tracking data on atmospheric passage (Popova et al. 2010). The recovered mass is smaller than estimated total fallen mass partially due to incomplete finding. The highest fractions are obtained for two smallest and slowest meteorites (~10%, Lost City and Innisfree), the smallest fractions ($<10^{-4}$)

are found for Tagish Lake and Almahata Sitta meteorites, probably due to their specific structure and composition.

The Tagish Lake material is classified as ungrouped carbonaceous chondrite with a very high porosity of 25-49%, and the largest meteorite fragment constitutes only about 10^{-5} of its initial meteoroid mass (Hildebrand et al. 2006). Modeling efforts done to describe the entry of the Tagish Lake meteoroid demonstrated that about of 80-90% of instantaneous mass of the body was lost in the main breakup at the altitude of about 34-35 km (Brown et al. 2002b; Ceplecha 2007). Hildebrand et al.(2006) concluded that most of the initial meteoroid mass (~60-90 t) was deposited at 30-40 km altitude as the dust. Attempts to apply pan-cake and progressive fragmentation models to the Tagish Lake case also confirmed that essential amount of its mass was deposited as the dust in the atmosphere similar to Almahata Sitta case. About 1000 kg of initial mass may be converted into meteorites. This estimate is of the same order as the mass estimates at the end of luminous trajectory (~1300 – 2700 kg) obtained by Brown et al.(2002) and Ceplecha (2007). Hildebrand et al.(2006) estimated the total fallen mass as about 100-1000 kg, and only 16.3 kg was collected.

Borovička and Charvat (2009) compared the apparent strengths at fragmentation for a few bolides and suggested that the Tagish Lake meteoroid is the best analog to asteroid TC$_3$ 2008. Presence of non-ureilite fragments among retrieved samples of Almahata Sitta shows inhomogeneous structure of the asteroid body (Bischoff et al. 2010). Besides, some authors suggest high macroporosity of TC$_3$ 2008 (Borovička and Charvat 2009; Welten et al. 2010; Kohout et al. 2010). The parent bodies of Tagish Lake and Almahata Sitta meteorites were probably very fragile and inhomogeneous. They were catastrophically disrupted during the atmospheric passage producing dust clouds, and their stronger parts became meteorites.

The opposite case was observed in the Carancas event, where the fall of a stony meteorite caused the formation of a 13-m wide impact crater. This ordinary chondrite meteoroid probably did not experienced significant atmospheric fragmentation (Borovička and Spurny 2008), although there was no detailed observational data. The meteoroid mass was estimated as about M~1300-10000 kg (Borovička and Spurny 2008) or even as 10000-50000 kg. (Kenkmann et al. 2009). The Carancas event confirms that meteoroid strength and fragmentation scenario can vary significantly from case to case. But it should be noted here that small crater formation on the Earth is an extremely rare event due to disruption of meteoroids in the atmosphere, whereas 10-30 similar sized bodies enter the atmosphere every year (Nemtchinov et al. 1997; Brown et al. 2002a).

3.3 Mbale

If the fraction of initial mass recovered as meteorites f_m exceeds about 1-5%, probably there is no large dust deposition during the passage. Entry of these meteoroids is reasonably described in the frame of progressive fragmentation models. Comparison of model predictions with strewn fields permits better understanding of the details of meteoroid breakups, although in many cases the incomplete recovery adds uncertainties in strewn field data.

About 150 kg of material in more than 850 pieces were collected on a strewn field of a size 3x7 km after the fall of L5/6 ordinary chondrite Mbale in 1992 (Jenniskens et al. 1994). Its pre-entry mass was estimated as 400-1000 kg (more probably ~1000 kg) based on cosmogenic radionuclide data. Entry velocity was roughly estimated as 13.5 km/s. It was assumed that small fragmentation started probably above 25 km, but the main catastrophic breakup occurred at 10-14 km altitude.

Application of progressive fragmentation model to the Mbale entry allowed estimation of fallen mass as 200-250 kg in 100-3000 fragments (in dependence on assumed breakup model) covering a

strewn field of about 1x7-9 km. Wind drift, which is essential for gram-sized fragments, wasn't taken into account. Multiple breakups occurred at the altitudes 22-35 km under the loading of about 0.8-1.3 MPa. Strength scaling law (with allowed random strength deviations) was used. The values of breakup loading are in the same range as for other observed meteoroid fragmentations (Popova et al. 2010), but it should be noted here that observed strength of meteoroids at breakup substantially deviates from this scaling law (Popova et al. 2010). The Mbale meteorite fragment distribution is better reproduced if a number of pieces following power law distribution are formed in every breakup. Model results satisfactorily describe the observed strewn field.

More strewn fields should be modeled in the future in order to better understand the details of the breakup process (strength at breakup; fragment distribution at breakup, etc).

4 Summary

Different fragmentation scenarios occur during the passage of meteoroids $100 - 10^6$ kg through the atmosphere. There are a number of events which deposited essential fraction of their masses as dust in the atmosphere. Observational data are still incomplete to make definite conclusion, what fraction of incoming bodies is fragile enough to deposit this dust and how it is related with their structure/composition etc. But even bodies, which deposited much of mass as a dust/vapor, are able to produce meteorites. The total picture of fragmented-body motion is comparatively complicated. Better statistics are needed to estimate parameters of incoming cosmic material and to predict its behavior in the atmosphere. A full set of data, including detailed light curves, photographic trajectories, spectra, acoustic and seismic signals, and data on the composition of found meteorites are highly desirable.

References

Artem'eva N.A., Shuvalov V.V. 1996. Interaction of shock waves during passage of disrupted meteoroid through atmosphere. Shock Waves 5, 359–367.

Artemieva, N.A., Shuvalov, V.V., 2001. Motion of a fragmented meteoroid through the planetary atmosphere. J. Geophys. Res. 106, 3297-3310.

Baldwin, B., Sheaffer, Y., 1971. Ablation and breakup of large meteoroids during atmospheric entry. J. Geophy. Res. 76, 4653-4668.

Bischoff, A., Horstmann, M., Laubenstein M.,Haberer, S. 2010. Asteroid 2008 TC3 – Almahata Sitta: not only a ureilitic meteorite, but a breccias containing many different achondritic and chondritic lithologies. Lunar Planet. Sci. 41. Abstract 1763

Bland, P.A., Artemieva, N.A., 2006. The rate of small impacts on Earth. Meteorit. Planet. Sci. 41, 607-631.

Borovička, J., Popova, O.P., Nemtchinov, I.V., Spurný, P., Ceplecha, Z., 1998. Bolides produced by impacts of large meteoroids into the Earth's atmosphere: comparison of theory with observations. I. Benesov bolide dynamics and fragmentation. Astron. Astrophys. 334, 713-728.

Borovička, J., Kalenda, P., 2003. The Morávka meteorite fall: 4. Meteoroid dynamics and fragmentation in the atmosphere. Meteorit. Planet. Sci. 38, 1023-1043.

Borovička, J., Spurny , P., 2008. The Caranacas meteorite impact – encouter with a monolithic meteoroid. Astron.Astrophys. 485, L1-L4.

Borovička, J., Charvat Z., 2009. Meteosat observation of the atmospheric entry of 2008 TC3 over Sudan and associated dust cloud. Astron.Astrophys. 485,1015-1022.

Boslough, M.B., Crawford, D.A., Robinson, A.C., et al.: Mass and Penetration Depth of Shoemaker-Levy 9 Fragments from Time-Resolved Photometry, GRL, 21, 1555–1558, 1994.

Britt, D.T., Consolmagno, G.J., 2003. Stony meteorite porosities and densities: a review of the data through 2001. Meteorit. Planet. Sci. 38, 1161-1180.

Brown, P., Spalding, R.E., ReVelle, D.O., Tagliaferri, E., Worden, S.P., 2002a. The flux of small near-Earth objects colliding with the Earth. Nature 420, 294-296.

Brown, P.G., ReVelle, D.O., Tagliaferri, E., Hildebrand, A.R., 2002b. An entry model for the Tagish Lake fireball using seismic, satellite and infrasound records. Meteorit. Planet. Sci 37, 661-675.

Carr M.H., 1970, Atmospheric collection of debris from the Revelstoke nd Allende fireballs. Geochimica et Cosmochimica Acta 34,689-700.

Ceplecha, Z., ReVelle, D.O.. 2005. Fragmentation model of meteoroid motion, mass loss, and radiation in the atmosphere. Meteorit. Planet. Sci. 40, 35-54.

Ceplecha Z., Spurný P., Borovička J., Keclíková J. 1993. Atmospheric fragmentation of meteoroids, Astron. Astrophys. 279, 615-626.

Ceplecha, Z., Borovička, J., Elford, W.G., ReVelle, D.O., Hawkes, R.L., Porubčan, V., Šimek, M., 1998. Meteor phenomena and bodies. Space Sci. Reviews 84, 327-471.

Fujiwara A., Cerromi P., Ryan E. et al. 1989. Experiments and scaling laws for catastrophic collisions. In: Asteroids II, eds.R.Binzel, T.Gehrels and M.Matthews, Univ.Arizona Press, Tucson, Arizona, 240-265.

Golub', A.P., Kosarev, I.B., Nemtchinov, I.V., Shuvalov, V.V., 1996. Emission and ablation of a large meteoroid in the course of its motion through the Earth's atmosphere. Solar System Res. 30, 183-197.

Hartmann, W.K., 1969. Terrestrial, Lunar, and Interplanetary Rock Fragmentation. Icarus 10, 201.

Hildebrand, A., McCausland, P.J.A. , Brown, P.G. , Longstaffe, F.J. , Russell, S.D.J. , Tagliaferri, E., Wacker, J.F., Mazur, M.J. , 2006. The fall and recovery of the Tagish Lake meteorite. Meteorit. Planet. Sci. 41, 407-431.

Hills J.G., Goda M.P. 1993. The fragmentation of small asteroids in the atmosphere. Astron. J.,105, 1114-1144.

Jenniskens P, Betlem H, Betlem J et al. 1994. The Mbale meteorite shower. Meteoritics 29,246–254.

Jenniskens P., and 34 colleagues, 2009. The impact and recovery of asteroid 2008 TC3. Nature. 458, 485-488.

Kenkmann T., Artemieva N.A., Wunnemann K., Poelchau M.H., Elbeshausen D., Nunes del Prado H., 2009. The Carancas meteorite impact crater, Peru: Geologic surveying and modeling of crater formation and atmospheric passage. Meteorit. Planet. Sci. 44, 985-1000.

Klekociuk A.R., Brown P.G., Pack D.W., ReVelle D.O., Edwards W.N., Spalding R.E., Tagliaferri E., Yoo B.B., Zagari J. 2005. Meteoritic dust from the atmospheric disintegration of a large meteoroid . Nature, 436,1132-1135.

Kohout T., Kiuru R., Montonen M., Scheirich P., Britt B., Macke R. Consolmagno G., 2010. 2008 TC3 asteroid internal structure and physicalproperties inferred from study of the Almahata Sitta meteorites. Icarus, under review.

Levin, B. Yu (1956) Fizicheskaya teoriya meteorov i meteornoe veshchestro v Solnechnoi sisteme (Physical Theory of Meteors and Meteoric Matter in the Solar System) Nauka, Moscow, 294 (in Russian)

McCord T.B., Morris J. Persing D. et al. Detection of a meteoroid entry into the Earth's atmosphere on February 1, 1994. 1995. JGR, 100, 3245-3249.

Nemtchinov, I.V., Popova, O.P., 1997. An analysis of the 1947 Sikhote-Alin event and a comparison with the phenomenon of February 1, 1994. Sol. Sys. Res. 31, 408-420.

Nemtchinov I.V., Svetsov V.V., Kosarev I.B. et al, 1997. Assessment of kinetic energy of meteoroids detected by satellite-based light sensors. Icarus, 130, 259–274.

Passey Q.R., Melosh H.J., 1980. Effects of atmospheric breakup on crater field formation. Icarus 42,211–233.

Popova, O., Nemchinov, I. 2008. Bolides in the Earth Atmosphere. In: Adushkin V., Nemchinov I. (Eds.). Catastrophic events caused by cosmic objects, Springer, pp.131-163.

Popova O., Borovička J., Hartmann W., Spurny P. et al. 2010. Very low strength of interplanetary meteoroids and small asteroids. Under review.

Svetsov, V.V., Nemtchinov, I.V., Teterev, A.V., 1995. Disintegration of large meteoroids in Earth's atmosphere: Theoretical models. Icarus 116, 131-153.

Shuvalov, V.V., Artemieva, N.N., 2002. Numerical modeling of Tunguska-like impacts. Planet. Space Sci. 50, 181-192.

Tsvetkov, V.I., Skripnik, A.Ya., 1991. Atmospheric fragmentation of meteorites according to strength theory. Astronom. Vestnik 25, 364-371 (in Russian).

Weibull, W.A., 1951. A statistical distribution function of wide applicability. J. Applied Mechanics 10, 140-147

Welten K.C., Meier M. M., Caffee M. W., Nishiizumi K., Wieler R., Jenniskens P., Shaddad M. H., 2010. High porosity and cosmic ray exposure age of asteroid 2008 TC3 derived from cosmogenic nuclides. Lunar Planet. Sci. 41. Abstract 2256.